Statistical analysis of Medium Scale Traveling Ionospheric Disturbances using the mid-latitude SuperDARN radars

Wataru Hazeyama[1], Nozomu Nishitani[1], Tomoaki Hori[1],
Takuji Nakamura[2], Septi Perwitasari[3]

1. ISEE, Nagoya University 2. NIPR 3. NICT

Traveling ionospheric disturbances (TIDs)

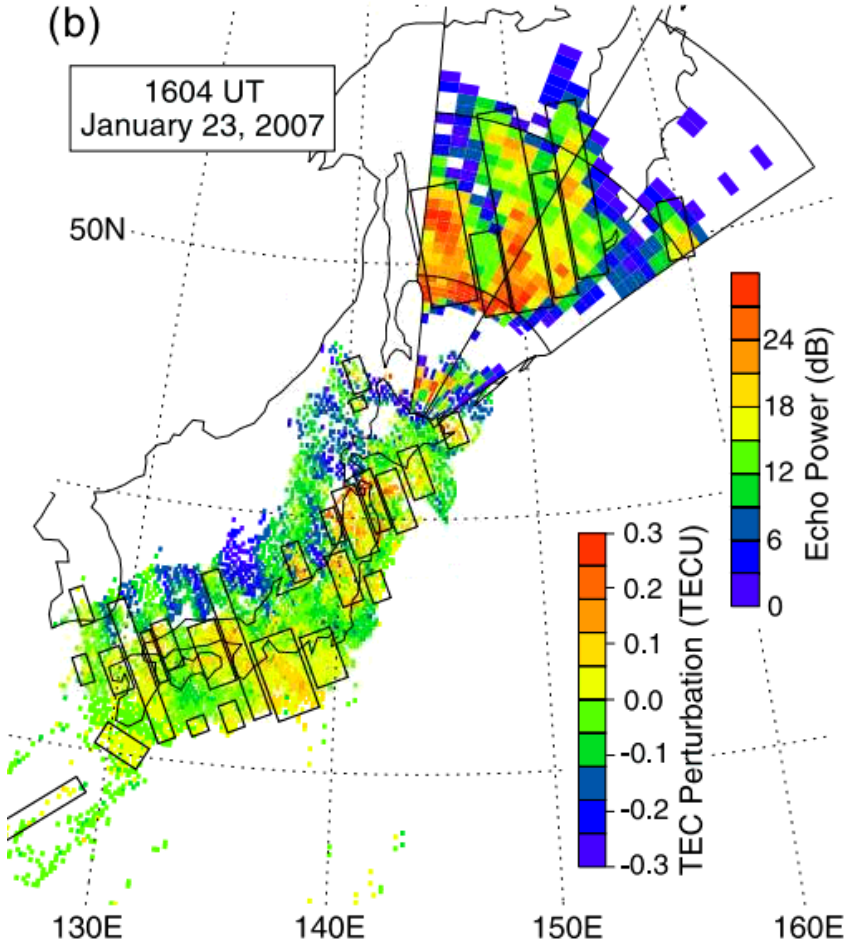

MSTID [Ogawa et al., 2009]

TIDs are the propagating wave-like electron density disturbances in the ionosphere. In particular, those with a **wavelength of several hundred kilometers** and a **period of 15 to 60 minutes** are called Medium-Scale TIDs (MSTIDs) [Hunsucker, 1982].

	Daytime MSTIDs	Nighttime MSTIDs
Origin	**Atmospheric gravity waves (AGWs)** [Hines 1960; Hooke,1968]	**Perkins instability** [Shiokawa et al., 2003b; Otsuka et al., 2004]
Propagation direction (Northern Hemisphere)	**Equatorward** [Ogawa et al., 2009]	**Southwestward** [Kotake et al., 2007; Yokoyama et al., 2009] Northward [Ichihara et al., 2013]
Observation equipment	SuperDARN, GPS observation	SuperDARN, GPS observation, All-sky airglow imager

Target of this presentation

Generation of nighttime MSTIDs

In mid-latitudes, **the Perkins instability** is considered to contribute to the generation of nighttime MSTIDs.

1. **neutral winds *u*** blow in the southwest direction.
2. **Pedersen current *J*** is generated by the $u \times B$ F-region dynamo electric field.
3. The Pedersen current causes **polarization electric field *E*** due to the inhomogeneous conductivity structure associated with MSTIDs.
4. The polarization electric field moves ionospehric plasma vertically **($E \times B$ drift)**.

- NW–SE-aligned structure and southwestward propagation
- Polarization electric field fluctuations

Perkins instability

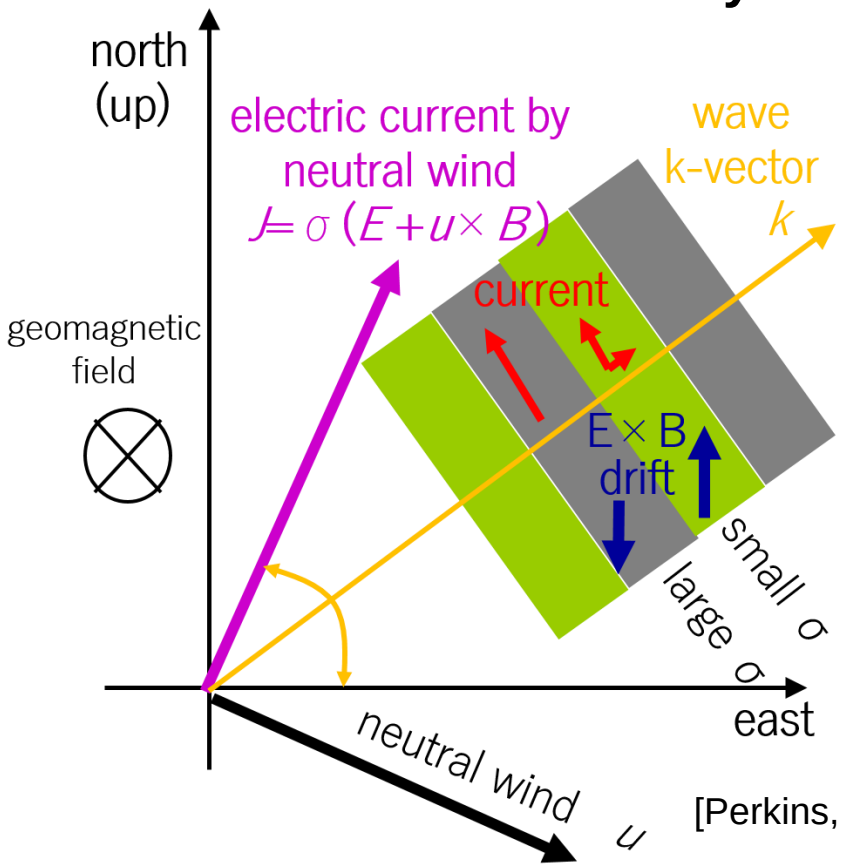

[Perkins, 1973]

MSTID observation by SuperDARN

- In the MSTID structure, **a polarization electric field is generated** due to the electron density disturbance.
- Due to the $\boldsymbol{E} \times \boldsymbol{B}$ drift, electron move to **opposite directions** at high and low electron densities.
- Because **the sign of the line-of-sight Doppler velocity is different** at high and low electron density, the MSTID can be observed by SuperDARN radars.

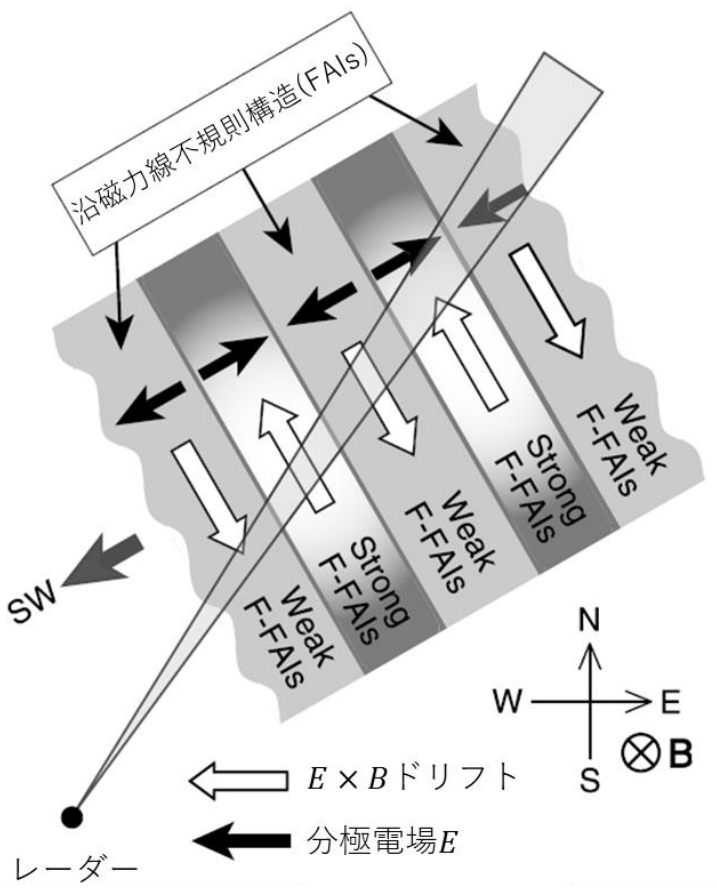

[Ogawa et al., 2009]

Solar activity dependence of MSTIDs

☐ Previous studies on solar activity dependence of MSTIDs

Paper	Location	Equipment	Relation	Notes
Amorim et al. (2011)	Brazil	All-sky imagers Ionosonde	Negative	
Oinats et al. (2016)	Hokkaido	SuperDARN radar	Positive	Daytime MSTID?
Tsuchiya et al. (2018)	Shiga Hokkaido	All-sky imagers	Negative	

☐ Problems

- The number of paper is small, and it is not clear that the correlation is **positive** or **negative**.
- The analyzed location is relatively small, and **the global characteristics are not clear**.
- There is no previous study which shows the solar activity dependence of **the polarization electric field fluctuation associated with nighttime MSTIDs**.

Method : 3-D FFT [Matsuda et al., 2014]

Determine the horizontal phase velocity and propagation direction of AGW from ground-based airglow images.

- **High-speed analysis** of large amount of data
- **No analyst bias**

Apply this method to the SuperDARN radar data to analyze MSTIDs

$$F(k_x, k_y, \omega) = \iiint V(x, y, t) \exp\left(-i\left(k_x x + k_y y + \omega t\right)\right) dx\, dy\, dt \quad (1)$$

$$v_x = \frac{\omega k_x}{k_x^2 + k_y^2} \quad (2), \qquad v_y = \frac{\omega k_y}{k_x^2 + k_y^2} \quad (3)$$

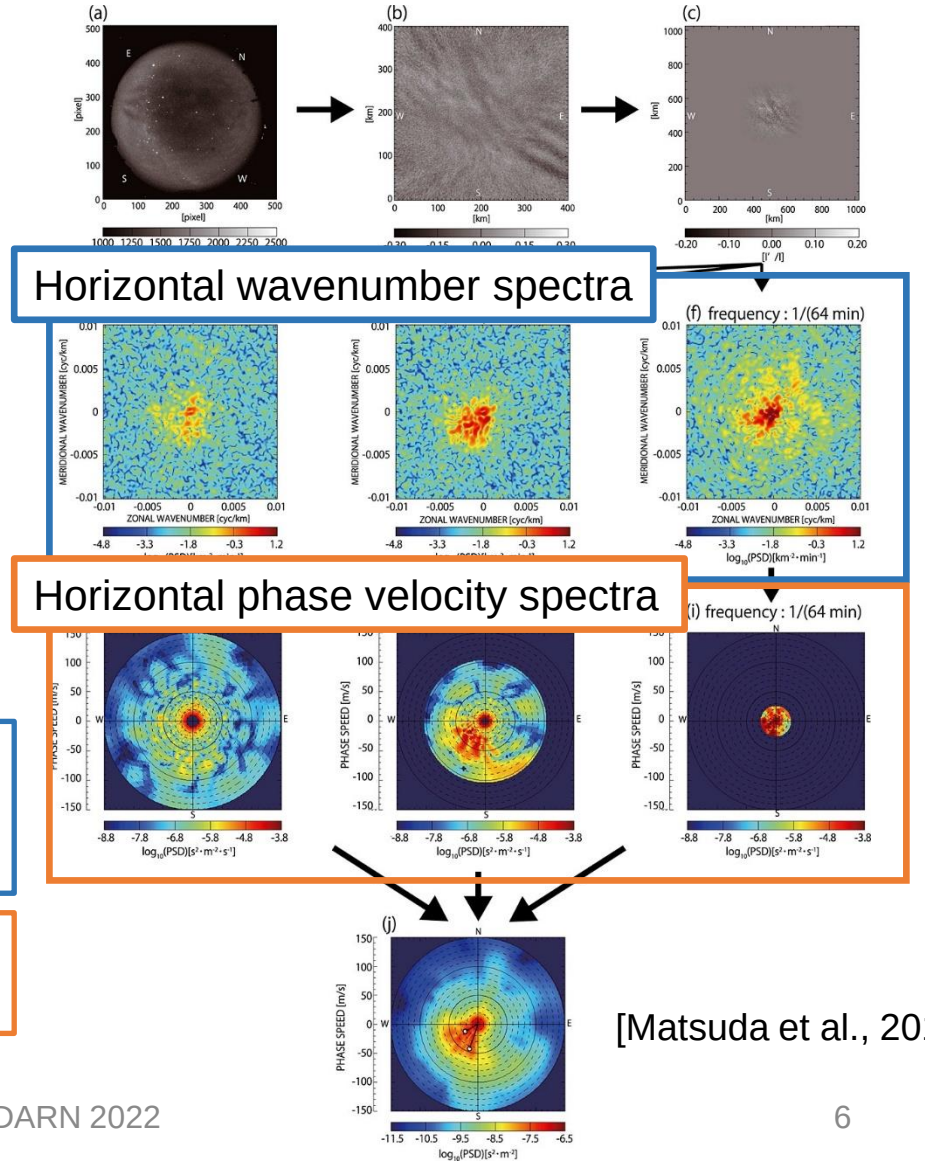

[Matsuda et al., 2014]

Dataset

Radar	Period	UT	G lat.	M lat.
Hokkaido East (HOK)	2009/01/01 – 2019/12/31	12:00 – 18:00	43.53°N	37.3°N
Hokkaido West (HKW)	2016/01/01 – 2019/12/31	12:00 – 18:00	43.53°N	37.3°N
Blackstone (BKS)	2012/01/01 – 2019/12/31	02:00 – 08:00	37.10°N	48.2°N
Fort Hays East (FHE)	2012/01/01 – 2019/12/31	04:00 – 10:00	38.86°N	48.9°N
Fort Hays West (FHW)	2012/01/01 – 2019/12/31	04:00 – 10:00	38.86°N	48.9°N
Christmas Valley East (CVE)	2012/01/01 – 2019/12/31	04:00 – 10:00	43.27°N	49.5°N
Christmas Valley West (CVW)	2012/01/01 – 2019/12/31	06:00 – 12:00	43.27°N	49.5°N

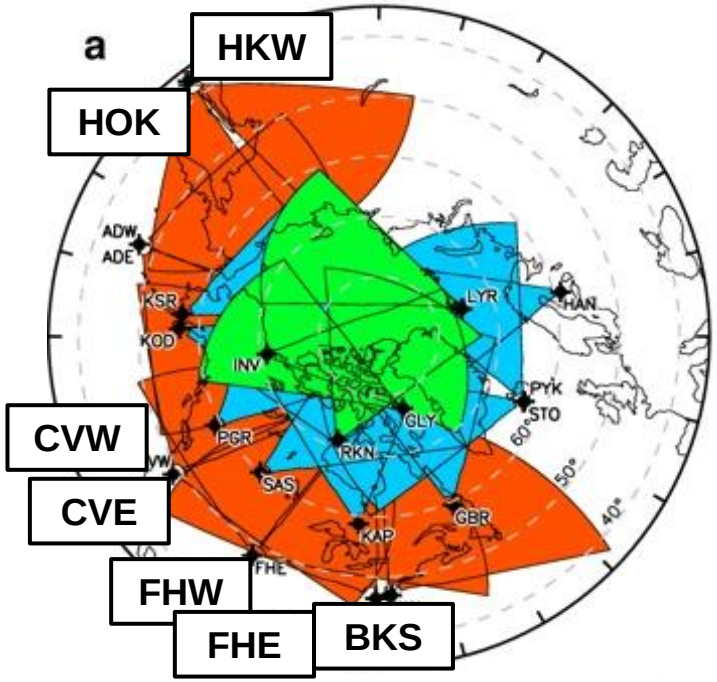

The SuperDARN radars' Field-of-view [Nishitani et al., 2019]

Solar activity … **F10.7 index**
[https://spaceweather.gc.ca/solarflux/sx-5-en.php]

Geomagnetic disturbance … **Hp30 index**
[https://www.gfz-potsdam.de/hpo-index/]

Results: How to Read a Plot

The distance from the center represents **the phase speed**.

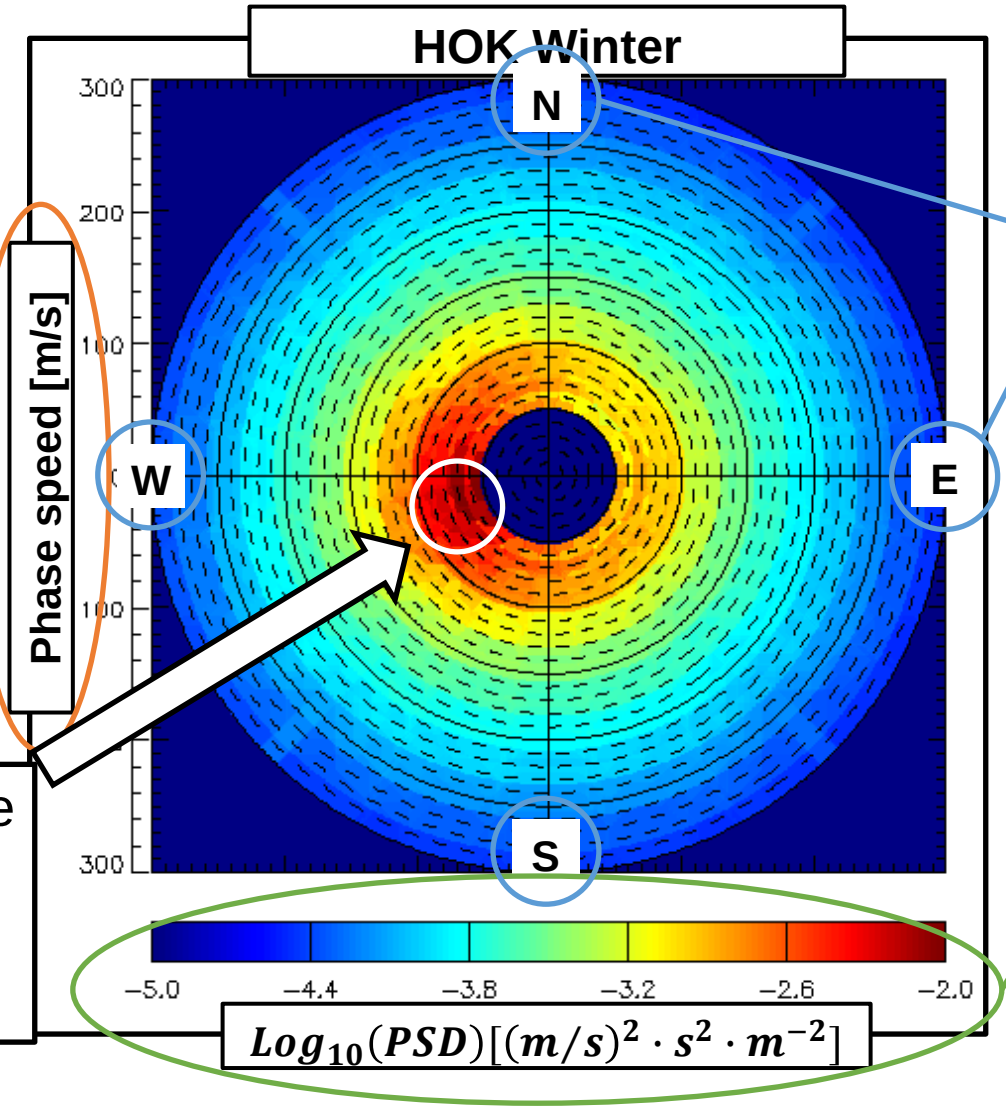

Each of the four sides represents **the propagation direction** (north at the top).

Many MSTIDs propagate **West-southwestward** during the analysis period.

Color bar represents **the power spectral density** (PSD), which depends on **the occurrence probability** and **amplitude** of MSTIDs.

Results: MSTID propagation

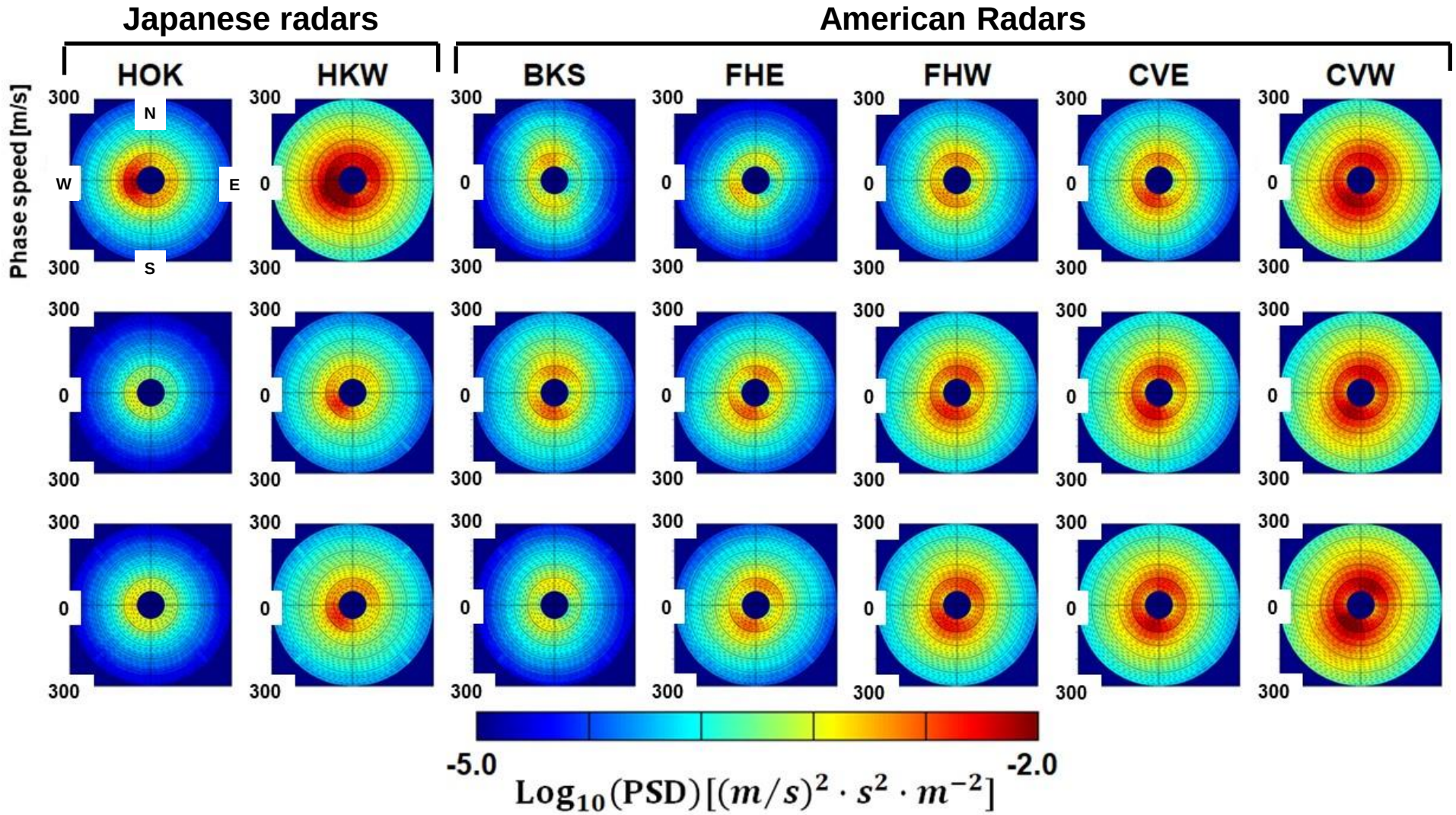

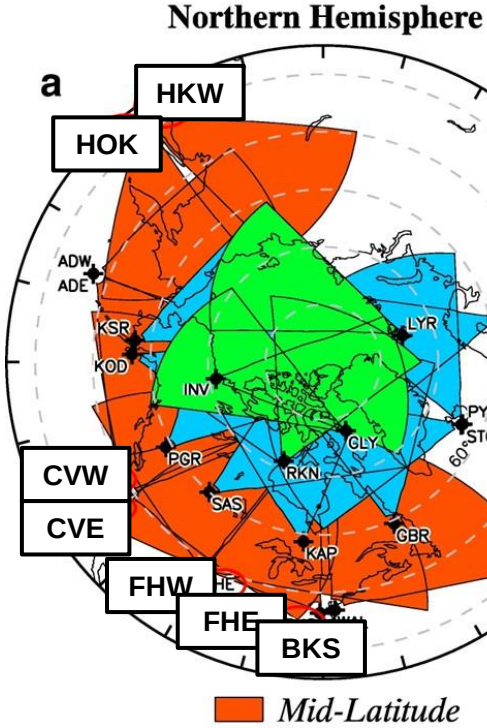

[Nishitani et al., 2019]

The PSD peak is positioned at the lower left of the plots.
→Mid-latitude MSTIDs mainly propagate **southwestward**.

Results: Solar activity dependence

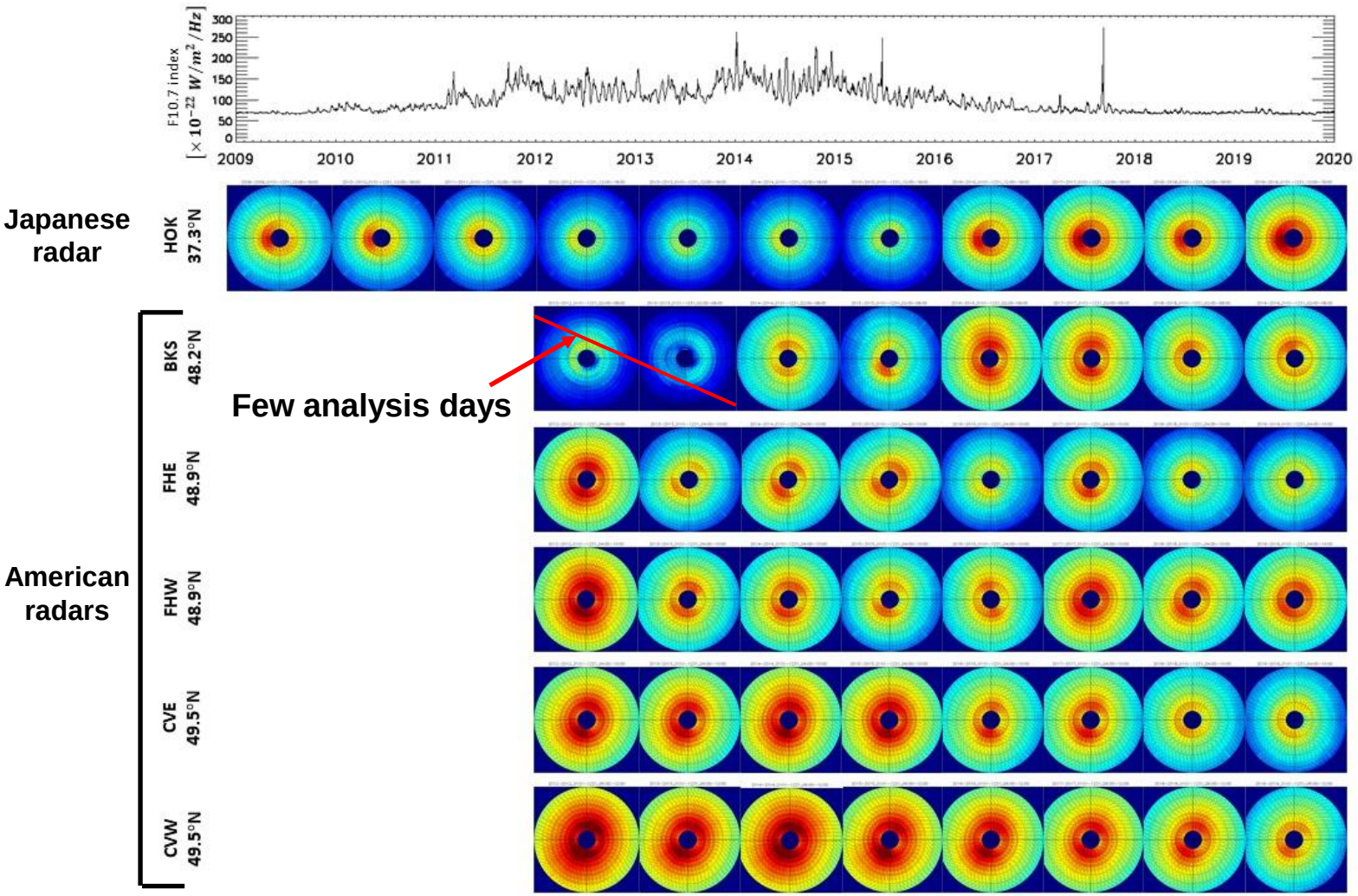

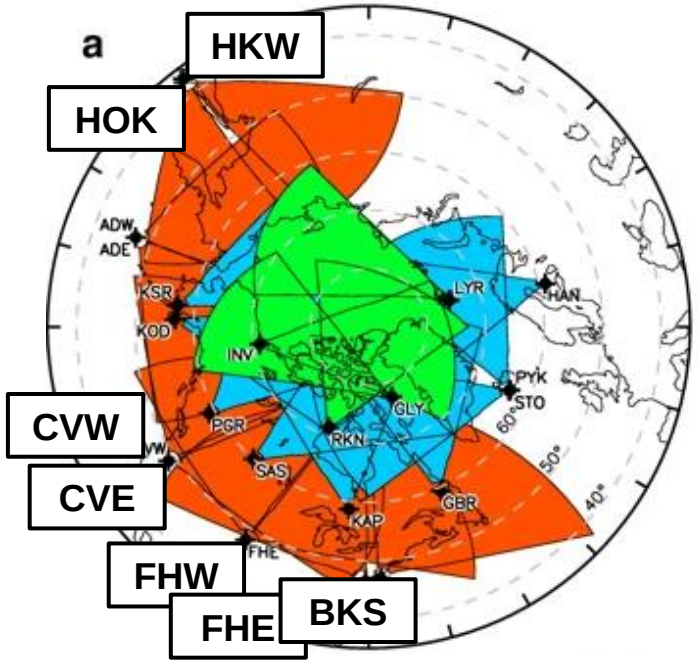

The SuperDARN radars' Field-of-view
[Nishitani et al., 2019]

The relation between average PSD and F10.7 Index is ...
Japanese sector: Negative
American sector: Positive

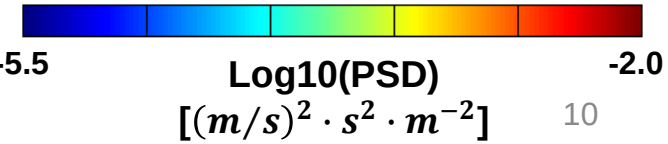

Results: Solar activity dependence

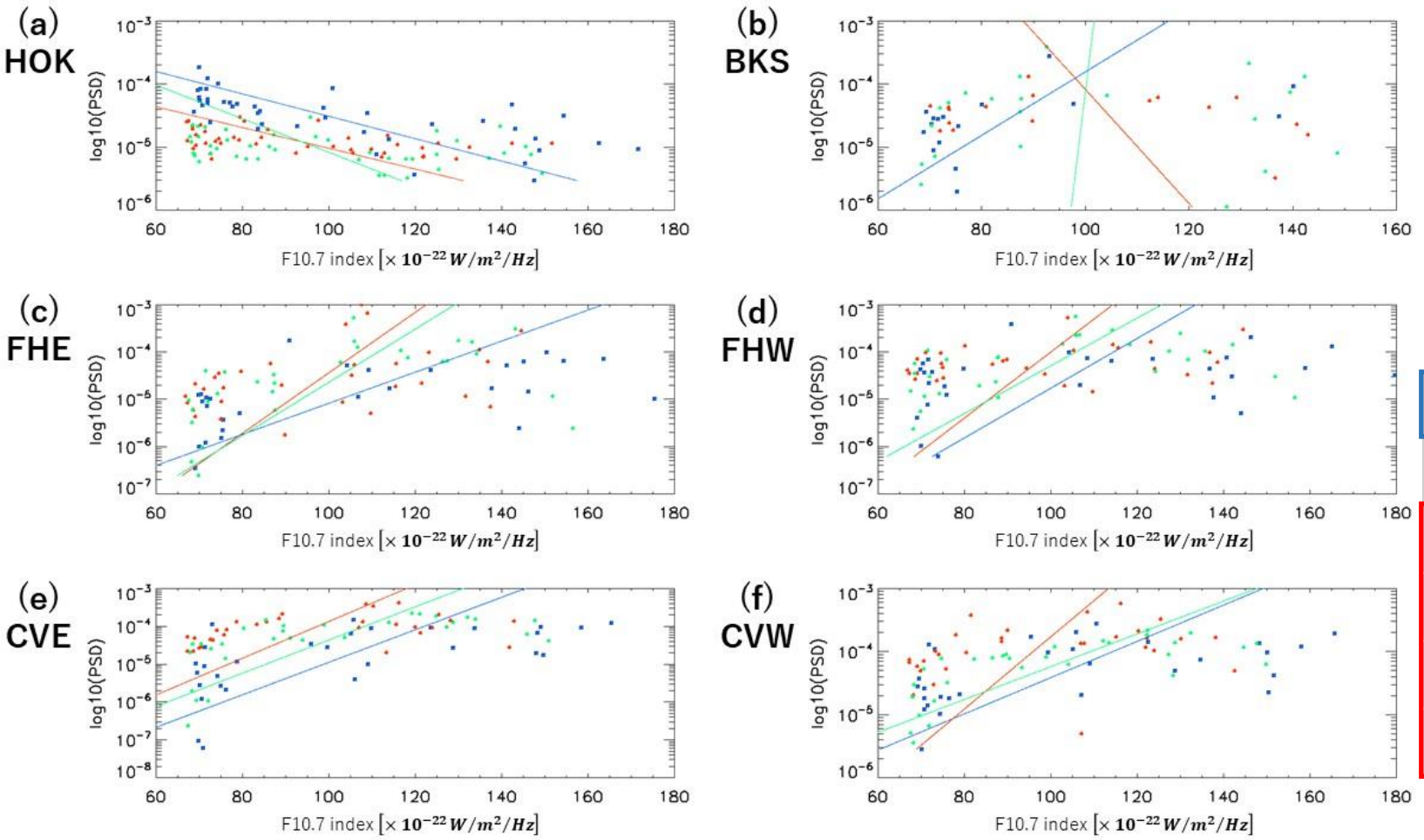

- Winter
- Equinox
- Summer

Correlation coefficient

	Winter	Equinox	Summer
HOK	-0.713	-0.326	-0.462
BKS	0.431	0.035	-0.114
FHE	0.562	0.517	0.417
FHW	0.329	0.399	0.241
CVE	0.619	0.618	0.432
CVW	0.540	0.682	0.381

Discussion

Japanese sector …
Southwestward propagation, **Negative correlation** with solar activity
North American sector …
Southwestward propagation, **Positive correlation** with solar activity

☐ **Propagation direction**
Waves with NW-SE wavefronts grow due to Perkins instability
→**Southwestward propagation**

Consistent with the results of many previous studies.
(e.g. Shiokawa et al., 2003; Ogawa et al., 2009; Otsuka et al., 2013)

☐ **Solar activity dependence**
Collision frequency of ions and neutral particles $\langle \nu_{in} \rangle$ and the scale height of the neutral atmosphere H_n have a **positive correlation** with solar activity.
→We can explain **the negative correlation** observed in Japan.

However, **the positive correlation** observed in North America **can't be explained by this theory.**
→**One possible factor is the difference of the magnetic latitude.**

Perkins instability

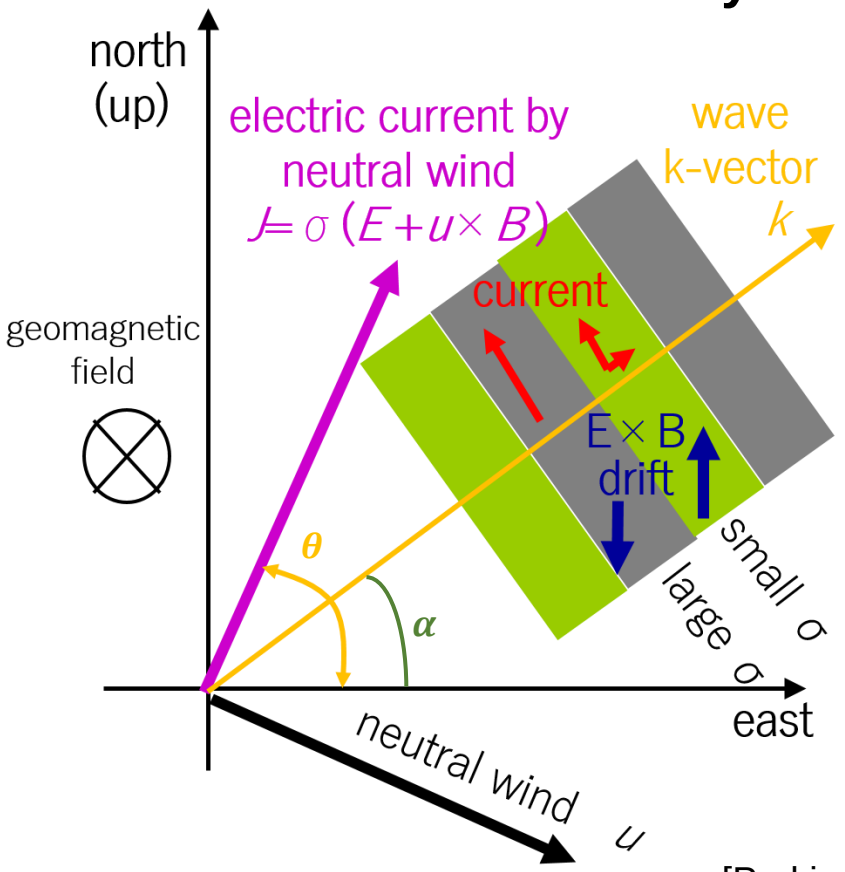

[Perkins, 1973]

The linear growth rate of Perkins instability

$$\gamma = \frac{g \sin^2 l}{\langle \nu_{in} \rangle H_n} \frac{\sin\alpha \sin(\theta - \alpha)}{\cos\theta}$$

Geomagnetic activity dependence

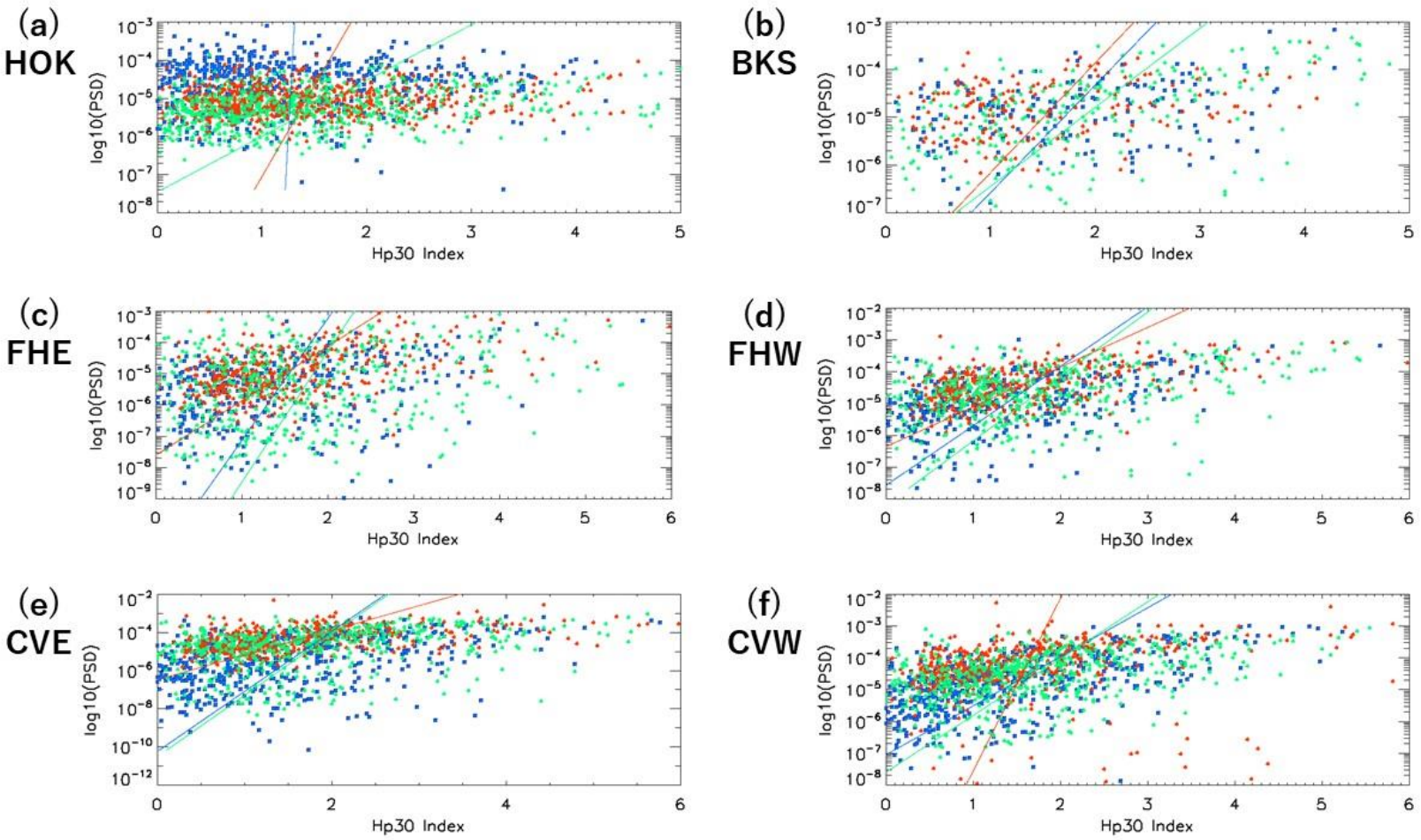

- Winter
- Equinox
- Summer

Correlation coefficient

	Winter	Equinox	Summer
HOK	0.014	0.305	0.085
BKS	0.297	0.480	0.263
FHE	0.275	0.248	0.445
FHW	0.458	0.357	0.488
CVE	0.382	0.299	0.452
CVW	0.558	0.400	0.161

Discussion: Relation with geomagnetic disturbances

Geomagnetic disturbances cause **enhancement of 2-cell convection**.

→**Additional poleward convection electric field E** occurs in the Dusk side mid-latitude regions.

→**Additional Pedersen current J**, under Perkins instability, leads to further enhancements of **MSTIDs.**

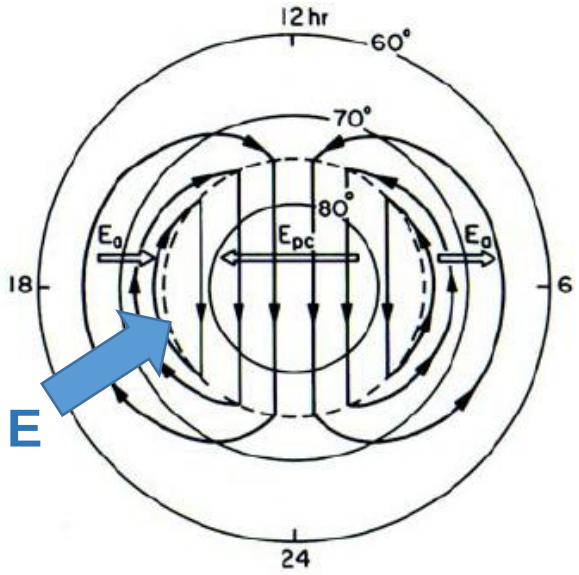

[Kelley, 1989]

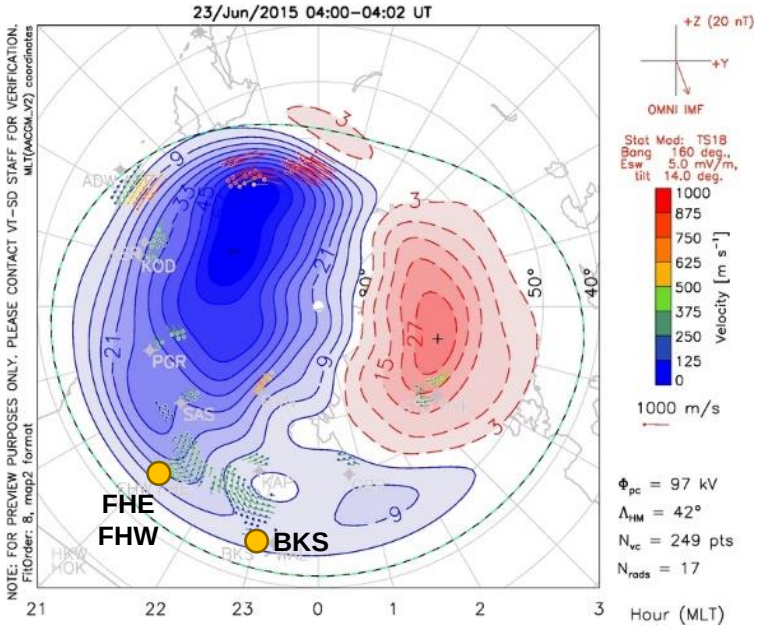

[http://vt.superdarn.org/tiki-index.php?page=DaViT+Map+Potential+Plot]

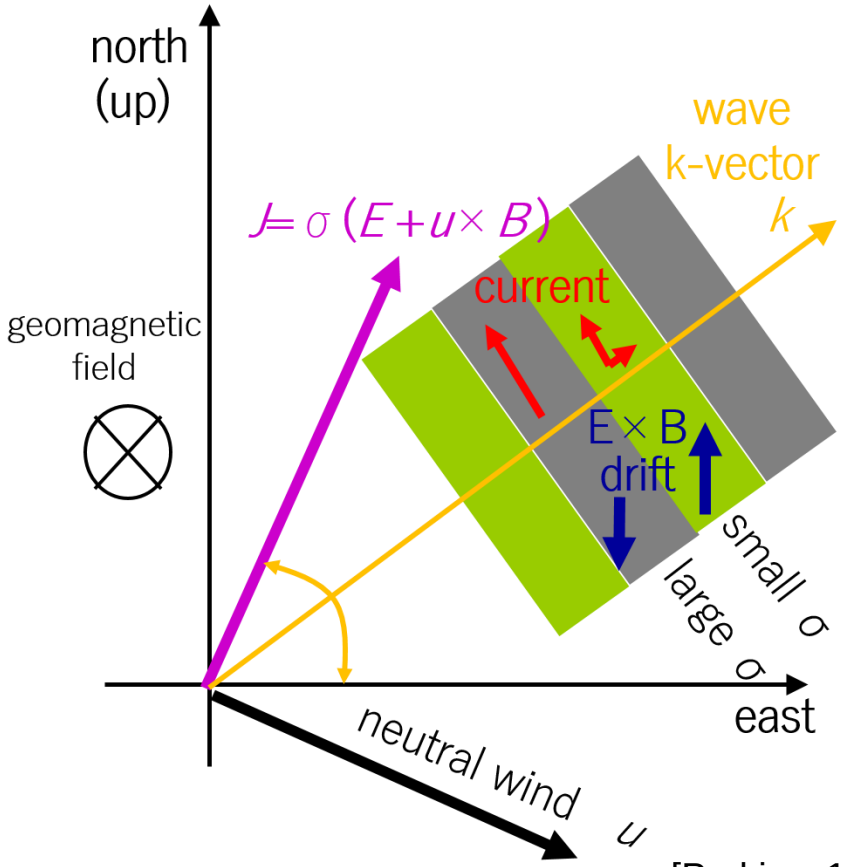

[Perkins, 1973]

Conclusion

We conducted **the statistical analysis of the characteristics of nighttime MSTIDs** using seven mid-latitude SuperDARN radars.

☐ Propagation direction

All radars observe **southwestward propagation**
→Consistent with the wavefront and propagation direction expected from the **Perkins instability**

☐ Solar activity dependence

- **Japanese sector** (M lat. : 37.3°N) … **Negative correlation**
  →Not affected by geomagnetic disturbance, and **can be explained by the linear growth rate of the Perkins instability**

- **North American sector** (M lat. : 48.2°N~49.5°N) … **Positive correlation**
  →**Geomagnetic disturbances generate additional poleward convection electric field**
  →**Intensified Pedersen currents**, under Perkins instability, lead to further enhancement **MSTIDs**

レーダー	冬（1, 2, 11, 12月）	春・秋（3, 4, 9, 10月）	夏（5, 6, 7, 8月）
HOK	552	615	693
HKW	369	483	462
BKS	171	231	179
FHE	346	436	400
FHW	331	421	381
CVE	496	508	474
CVW	544	554	505

	2009	2010	2011	2012	2013	2014	2015	2016	2017	2018	2019
HOK	156	147	151	151	105	157	85	156	281	195	275
BKS				6	3	72	19	121	170	128	62
FHE				180	60	138	78	118	208	155	245
FHW				181	58	137	50	115	203	155	234
CVE				167	182	259	111	174	197	182	206
CVW				226	197	262	114	171	194	191	248

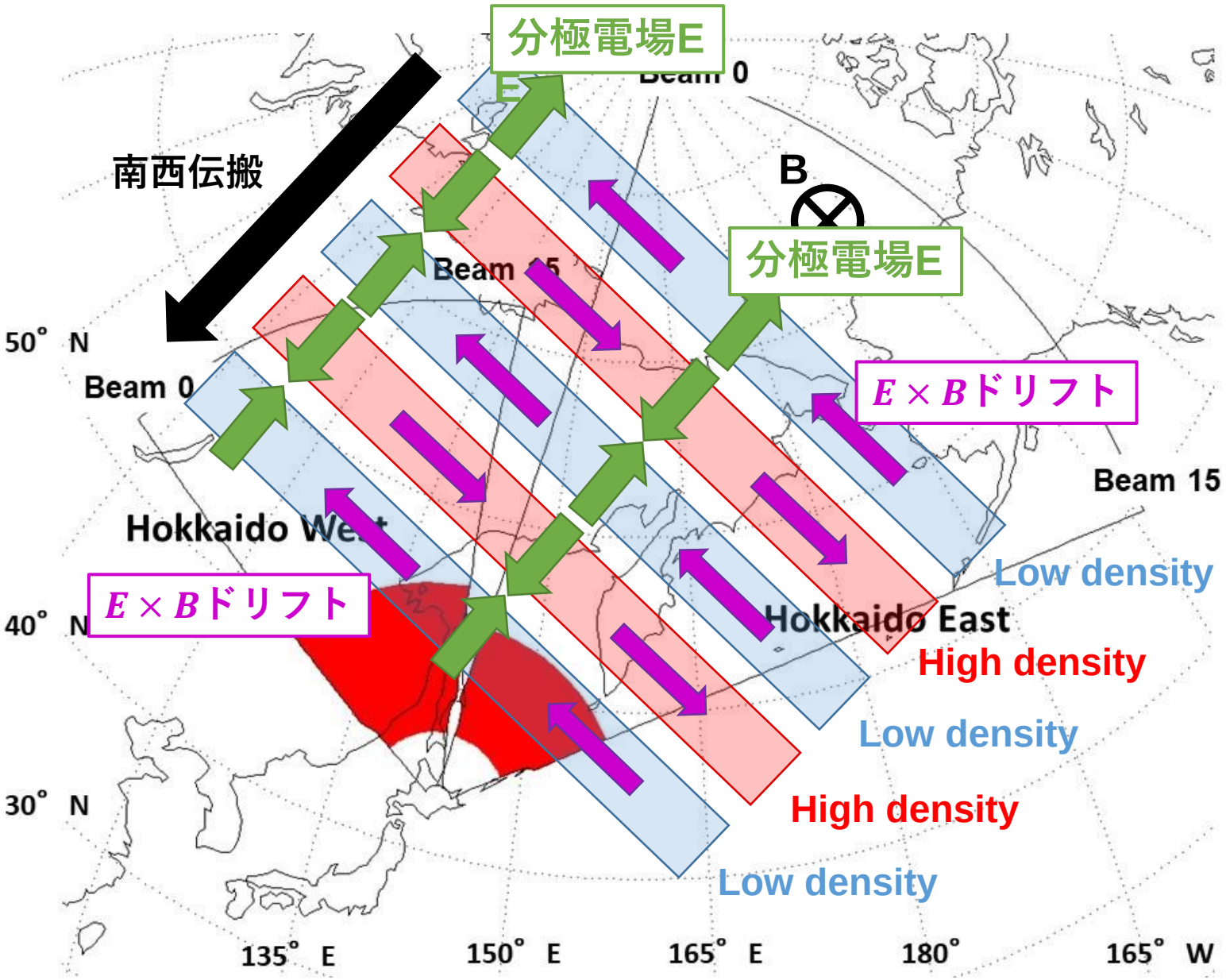

Doppler 速度 (LOS成分)
HOK…小
HKW…大

Results: Event analysis

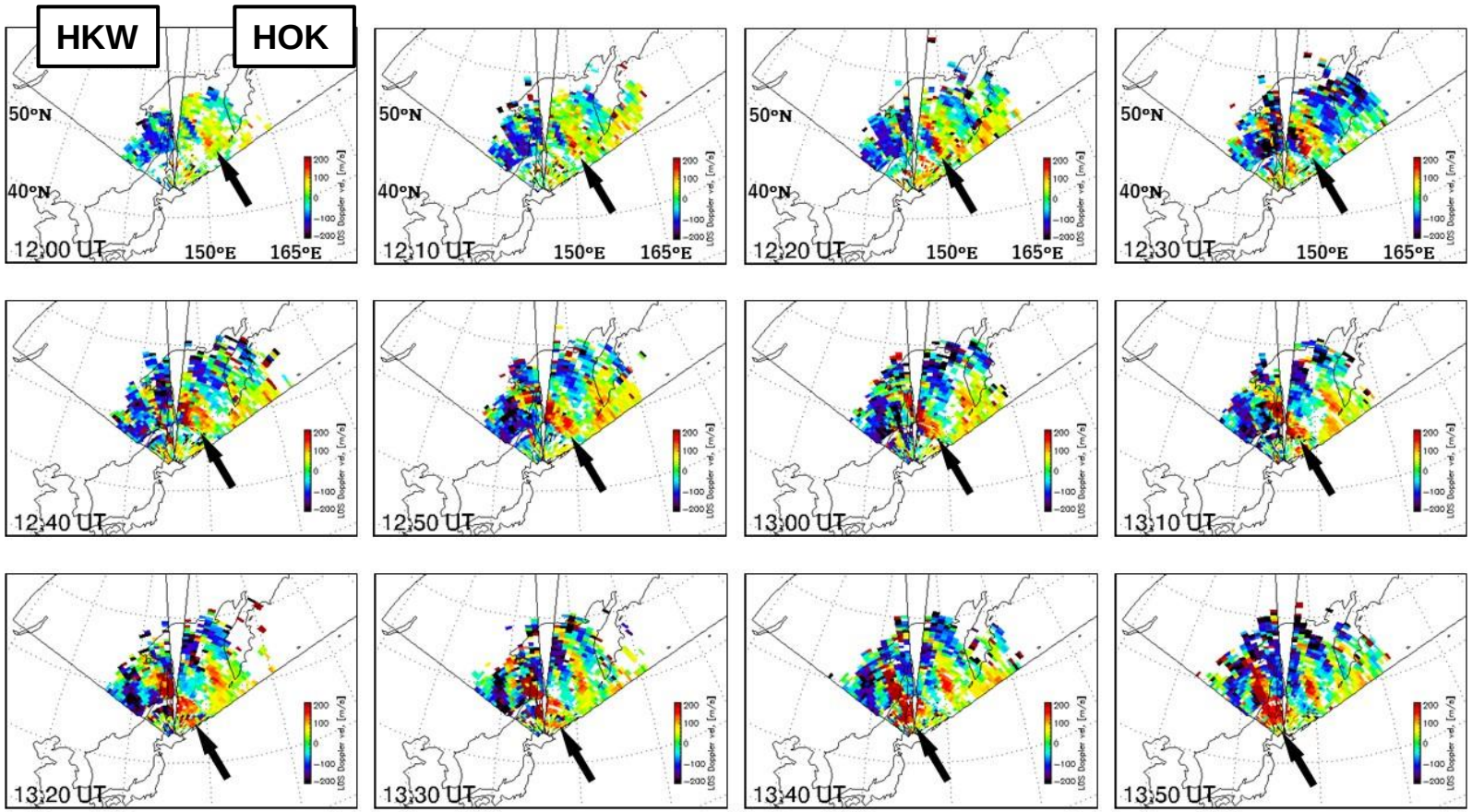

Event: 2019-01-12 / 12:00-14:00 (UT)